Fabrication of a Gradient Heterogeneous Surface Using Homopolymers and Diblock Copolymers

Irene Y. Tsai,[†] Masahiro Kimura,[‡] and Thomas P. Russell*,[†]

Polymer Science and Engineering Department, University of Massachusetts, Amherst, Massachusetts 01003, and Films & Film Products Research Laboratories, Toray Industries, Inc., 1-1 Sonoyama 1-chome, Otsu, Shiga 520-8558, Japan

Received January 6, 2004. In Final Form: April 19, 2004

The strength of the interfacial interactions and the length scale over which these interactions occur are key factors in understanding the thin film behavior of polymer blends and diblock copolymers, adhesion, wettability, and recognition processes of cells and random heteropolymers on surfaces. Here, gradient heterogeneous surface topographies were prepared using thin films of mixtures of homopolymers and diblock copolymers to vary the lateral size scale of heterogeneities from the microscopic to nanoscopic. Dewetting, phase separation, and cell adhesion were used to demonstrate the utility of these surfaces having gradient heterogeneous topographies. By tuning the lateral size scale of the heterogeneities, surface patterns can be engineered to meet a specific function. Gradient surfaces offer a straightforward method to optimize various length scales of heterogeneity.

Introduction

The strength and lateral distribution of interfacial interactions govern morphologies in thin films of polymer blends[1−4] and diblock copolymers,[5−8] dictate recognition processes of cells[9−14] and random heteropolymers,[15] and can be used to control adhesion[16] and surface wettability.[17] The lateral length scale over which a thin film of a homopolymer mixture phase separates on a chemically patterned surface provides a simple example of this.[3] Recognition on a very-coarse-grained level is seen by the behavior of block copolymers on patterned surfaces.[18−20] Many biological processes rely on protein recognition of a specific pattern of interacting sites on a surface.[14] A simple means of examining patterns and the influence of patterns on many length scales simultaneously is with gradient surfaces, where lateral correlations in the chemical nature and functionality of the surface can be varied in a systematic manner.[21−23]

Heterogeneous surfaces with a gradient in length scale from the nanoscopic to the microscopic can be fabricated using mixtures of homopolymers with diblock copolymers. Mixtures of homopolymers, in general, macroscopically phase separate, whereas diblock copolymers microphase separate on the nanoscopic length scale. Thus, by gradually varying the relative concentrations of homopolymers and block copolymers, the length scale of the domains can be continuously varied from the nanoscopic to the macroscopic. Here, a method to generate gradient surfaces based on such mixtures is described along with several examples demonstrating their utility.

Experimental Method

Asymmetric diblock copolymers of polystyrene, PS, and poly(methyl methacrylate), PMMA, denoted PS-*b*-PMMA with a molecular weight of 73 000 and a polydispersity of 1.04 were prepared in house by standard anionic polymerization methods. The volume fraction of PS in PS-*b*-PMMA is 0.7, and therefore, the equilibrium morphology of the copolymer is one with cylindrical microdomains of PMMA with an average separation distance of 30 nm. PS and PMMA with narrow molecular weight distributions and molecular weights of 52 000 and 29 000, respectively, were purchased from Polymer Laboratories and used without further purification. A hydroxy-terminated random copolymer of styrene and methyl methacrylate, denoted P(S-*r*-MMA), with a styrene fraction of 0.58 was prepared by a living free radical nitroxide mediated synthesis. This P(S-*r*-MMA) was anchored to the native oxide layer of a silicon substrate as described previously.[24] The interfacial interactions between the substrate and the PS and PMMA are balanced.

[†] University of Massachusetts.

[‡] Toray Industries, Inc.

(1) Krausch, G.; Kramer, E.; Rafailovich, M.; Sokolov, J. *Appl. Phys. Lett.* **1994**, *20*, 64.

(2) Seok, K.; Freed, F.; Szleifer, I. *J. Chem. Phys.* **2000**, *112*, 14.

(3) Böltau, M.; Walheim, S.; Mlynek, J.; Krausch, G.; Steiner, U. *Nature* **1998**, *391*, 877.

(4) Kielhorn, L.; Muthukumar, M. *J. Chem. Phys.* **1999**, *111*, 5.

(5) Petera; Muthukumar, M. *J. Chem. Phys.* **1997**, *107* (22), 9640.

(6) Fasolka, M. J.; Harris, D. J.; Mayes, A. M.; Yoon, M.; Mochrie, S. G. J. *Phys. Rev. Lett.* **1997**, *79*, *16*, 3018.

(7) Heier, J.; Genzer, J.; Kramer, E. J.; Bates, F. S.; Walheim, S.; Krausch, G. *J. Chem. Phys.* **1999**, *111*, *24*, 11101.

(8) Yang, X. M.; Peters, R. D.; Nealey, P. F.; Solak, H. H.; Cerrina, F. *Macromolecules* **2000**, *33*, 9575.

(9) Clark, P.; Connolly, P.; Curtis, A. S.; Dow, J. A.; Wilkinson, C. D. *Development* **1990**, *108*, 635−644.

(10) Flemming, R. G.; Murphy, C. J.; Abrams, G. A.; Goodman, S. L.; Nealey, P. F. *Biomaterials* **1999**, *20*, 573−388.

(11) Patel, N.; Padera, R.; Sanders, G. H.; Cannizzaro, S. M.; Davies, M. C.; Langer, R.; Roberts, C. J.; Tendler, S. J.; Williams, P. M.; Shakesheff, K. M. *FASEB J.* **1998**, *12*, 1447−1454.

(12) Whitesides, G. M.; Ostuni, E.; Takayama, S.; Jiang, X.; Ingber, D. E. *Annu. Rev. Biomed. Eng. 3*, 335−73.

(13) Mrksich, M.; Chen, C. S.; Xia, Y.; Dike, L. E.; Ingber, D. E.; Whitesides, G. M. *Proc. Natl. Acad. Sci. U.S.A.* **1996**, *93*, 10775−10778.

(14) Tirrell, M.; Kokkoli, E.; Biesalski, M. *Surf. Sci.* **2002**, *500* (1−3), 61−83.

(15) Bratko, D.; Chakraborty, A. K.; Shakhnovich, E. I. *Chem. Phys. Lett.* **1997**, *280*, 46−52.

(16) Golumbfskie, J.; Pande, V. S.; Chakraborty, A. K. *Proc. Natl. Acad. Sci.* **1999**, *96*, *21*, 11707−11712.

(17) Zope, M.; Kargupta, K.; Sharma, A. *J. Chem. Phys.* **2001**, *114*, 7211−7221.

(18) Rockford, L.; Liu, Y.; Mansky, P.; Russell, T. P.; Yoon, M.; Mochrie, S. G. J. *Phys. Rev. Lett.* **1999**, *82*, *12*, 2602.

(19) Rockford, L.; Mochrie, S. G. J.; Russell, T. P. *Macromolecules* **2001**, *34*, 1487.

(20) Kim, S. O.; Solak, H. H.; Stoykovich, M. P.; Ferrier, N. J.; de Pablo, J. J.; Nealey, P. F. *Nature* **2003**, *424*, 411.

(21) Meredith, J. C.; Smith, A. P.; Karim, A.; Amis, E. J. *Macromolecules* **2000**, *33*, 9747.

(22) Meredith, J. C.; Karim, A.; Amis, E. J. *Macromolecules* **2000**, *33*, 5760.

(23) Beers, K. L.; Douglas, J. F.; Amis, E. J.; Karim, A. *Langmuir* **2003**, *19* (9), 3935−3940.

10.1021/la049957w CCC: $27.50
Published on Web 06/11/2004

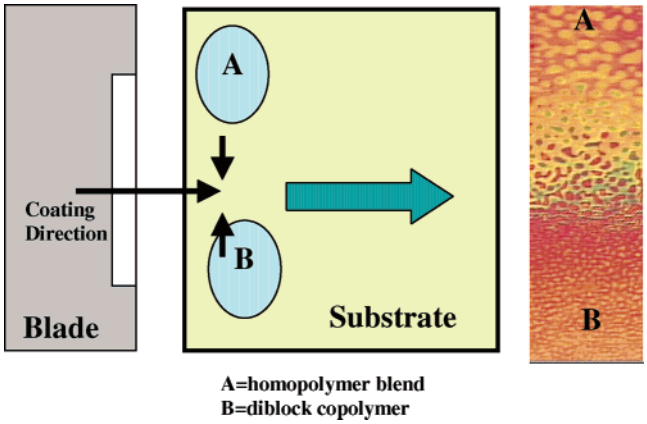

Figure 1. Schematic representation of the fabrication of gradient heterogeneous surfaces.

Eleven discrete samples of 1% solutions of PS-*b*-PMMA with different concentrations of PS and PMMA were prepared in toluene. The relative concentrations of the PS and PMMA were kept constant and the total concentration of the homopolymer was varied. In one set of experiments, the samples were annealed under vacuum for 48 h at 170 °C. In a second set of experiments, after the polymer film was dried, a layer of poly(dimethylsiloxane), PDMS, was spin coated onto the surface of the mixture and cross-linked at room temperature for 1 day. Consequently, the air surface was replaced with PDMS so that segregation of the components to this interface would be governed by the interaction energies among PS, PMMA, and PDMS. This bilayer was then annealed at 170 °C for 48 h. X-ray photoelectron spectroscopy measurements showed that, upon removal of the PDMS after annealing, there was no penetration of PDMS into the film.

Gradient surfaces were prepared by allowing two solutions, one a 0.5% solution of PS (52K) + PMMA (29K) in toluene and the other a 0.5% solution of PS-*b*-PMMA (70/30, 73K) in toluene, to wet a substrate and interdiffuse, creating a gradient in the concentration of the components.[21−23] Seconds after the solutions made contact, the solution was then blade coated normal to the gradient direction and the solvent was allowed to evaporate. This left a ∼30 nm thick film of polymer where the copolymer concentration was constant in the coating direction but varied continuously normal to this. Films were then annealed at 170 °C for 48 h under vacuum. This process is schematically shown in Figure 1.

All samples were reactive ion etched to remove the top ∼6 nm of the films. Subsequently, the films were exposed to ultraviolet radiation for 35 min to cross-link the PS and degrade the PMMA. The films were then washed for 3 min with acetic acid, rinsed with water, dried, and characterized by optical and scanning force microscopies. The autocorrelation functions of the images were obtained using Scion software[25] to determine the lateral length scale of heterogeneities in the films. The dewetting characteristics of PS (52K) and the phase separation behavior of mixtures of PS (52K) and PMMA (29K) were examined on the gradient heterogeneous surfaces.

Cells NIH_3T_3 were allowed to spread on discrete and gradient surfaces for 2 h. The samples were fixed in 0.25% glutaraldehyde for 1 min and then permeabilized in Karsenti's buffer (0.5% Triton X-100, 80 mM PIPES, 1 mM $MgSO_4$, 5 mM EGTA, pH 6.9) for 1 min, followed by an additional fixation in 0.5% glutaraldehyde for 10 min. The fixed cells on the surfaces were washed and stored in phosphate-buffered saline containing 0.1% Tween-20 and 0.02% sodium azide. To visualize F-actin, cells were incubated for 15 min in rhodamine-labeled phalloidin (Molecular Probes, Eugene, OR) following established procedures. Samples were washed extensively with phosphate-buffered saline placed between a glass slide and glass coverslips following the addition of ImmunoFluor mounting medium (ICN Biomedicals Inc., Irvine, CA). F-actin fluorescence was photographed using an Olympus BX51 reflection fluorescence microscope equipped with a digital camera. Images were acquired at 400× magnification and processed using Paintshop Pro software. The images shown are representative images of the cytoskeleton.

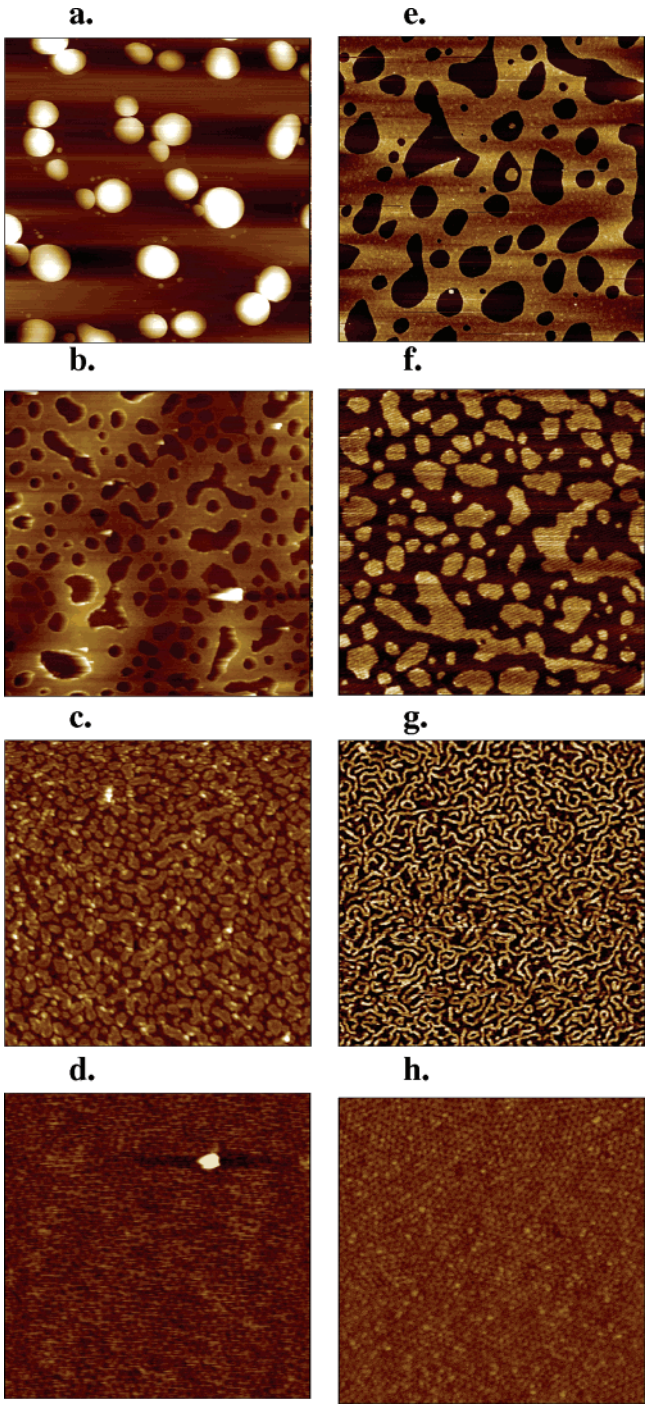

Figure 2. AFM images of films prepared from four different mixtures of PS, PMMA, and PS-*b*-MMA without (a−d) and with (e−h) a PDMS overlayer: (a) (PS + PMMA):P(S-*b*-MMA) = 1:0, (20 × 20 μm^2); (b) (PS + PMMA):P(S-*b*-MMA) = 0.8:0.2 (5 × 5 μm^2); (c) (PS + PMMA):P(S-*b*-MMA) = 0.6:0.4 (5 × 5 μm^2); (d) (PS + PMMA):P(S-*b*-MMA) = 0:1 (2 × 2 μm^2); (e) (PS + PMMA):P(S-*b*-MMA) = 1:0 (10 × 10 μm^2); (f) (PS + PMMA):P(S-*b*-MMA) = 0.7:0.3 (5 × 5 μm^2); (g) (PS + PMMA):P(S-*b*-MMA) = 0.5:0.5 (5 × 5 μm^2); (h) (PS + PMMA):P(S-*b*-MMA) = 0:1 (2 × 2 μm^2).

(24) Mansky, P.; Huang, E.; Liu, Y.; Russell, T. P.; Hawker, C. *Science* **1997**, *275*, 1458.

(25) Autocorrelation analysis was performed on a PC computer using the public domain NIH Image program (developed at the U.S. National Institutes of Health and available on the Internet at http://rsb.info.nih.gov/nih-image/), Scion software.

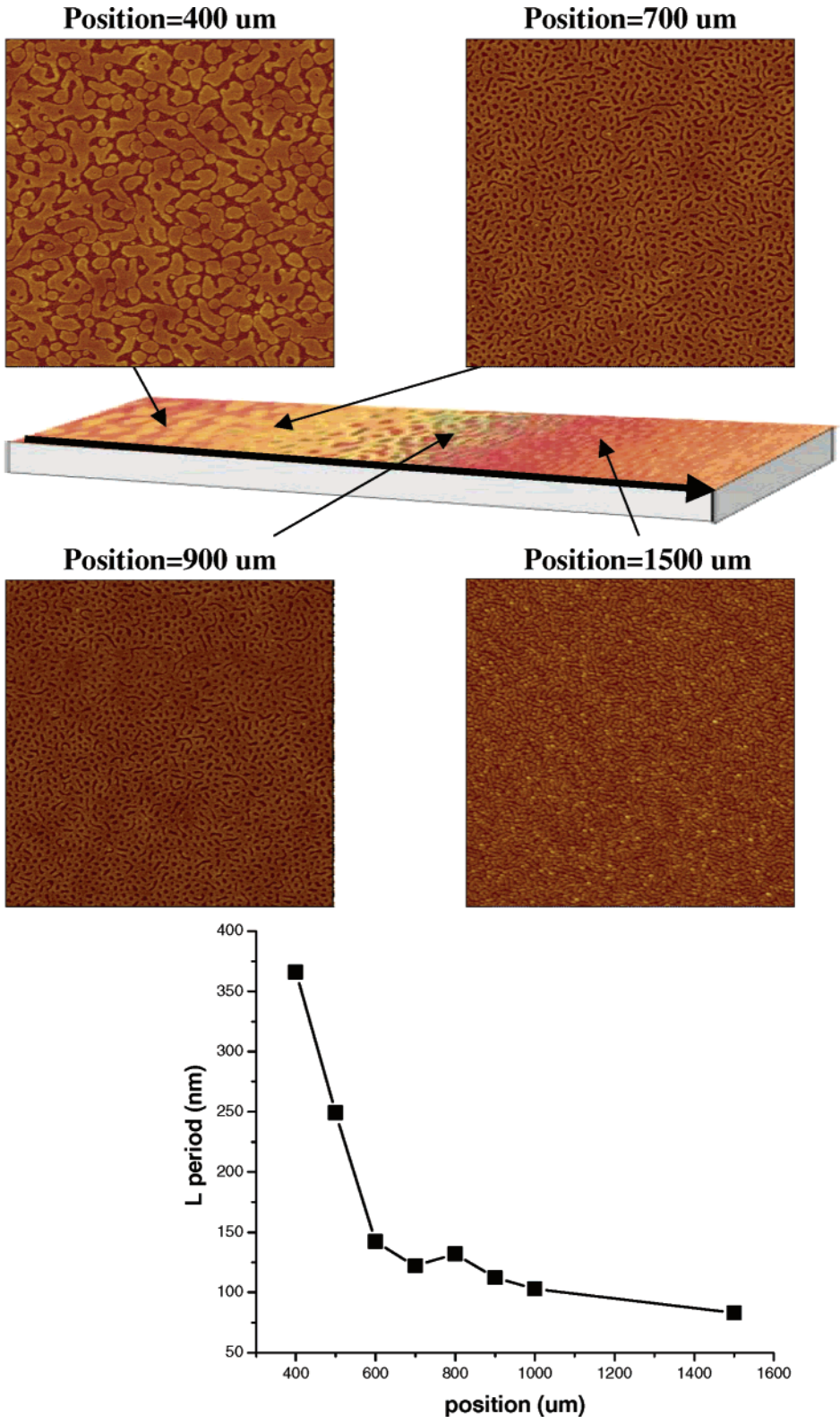

Figure 3. AFM images ($5 \times 5\ \mu m^2$) of gradient heterogeneous surfaces.

Results and Discussion

AFM images of films prepared from four different mixtures of PS, PMMA, and PS-*b*-PMMA with and without a PDMS overlayer are shown in Figure 2. As can be seen, as the concentration of the copolymer increases, the size scales of the heterogeneities decrease. The difference between the two preparations with and without the PDMS overlayer arise from the preferential segregation of PS, the lower surface energy component, to the air interface, which is absent when the PDMS is used. This surface segregation required the use of reactive ion etching with oxygen to remove the topmost ~6 nm of the film, thereby exposing the underlying morphology. It should be noted that reactive ion etching changes a flat PS surface from being hydrophobic to hydrophilic as evidenced by the change in the water contact angle from 90° to 10°. From

these images and, more quantitatively, from the correlation function of the images, the average size of the heterogeneities is seen to vary from ~30 nm for the copolymer to 6 μm for the mixture. Only slight differences in the correlation lengths were seen between the two different preparations, indicating that changes in the concentration due to surface segregation were not significant.

Gradient Heterogeneous Surface and Utilization. These discrete studies demonstrated the range in size scales of the morphologies that can be accessed with homopolymer/copolymer mixtures in thin films. A gradient surface was prepared by interdiffusing the homopolymer and copolymer solutions and then blade coating the gradient solution normal to the gradient. The AFM images in Figure 3 show the gradient in the morphology achieved by this approach.

The correlation function, determined from these images, yielded an average size scale of the heterogeneities that varied from 370 to 70 nm over a distance of ~1000 μm. This is shown in Figure 3. Measurements at the extreme ends of the film produced larger size scale structures for the pure homopolymer mixtures and smaller size scales for the pure copolymer. These are not shown, since the size scale of the morphology was sigmoidal in shape and only the region where large changes in the size scale was evident is discussed. Alternate routes to control the magnitude of the gradient in the size scale of the morphology are being developed by changing the concentration of the solution across the surface in a more systematic manner.[21−23] It should also be noted that the size scale of the morphology in the drawing direction did not vary appreciably over distances of several centimeters.

The dewetting of a 30 nm thick PS film (M_W = 52K) is used to illustrate the utility of these surfaces with a gradient in the morphology. The PS, as shown in Figure 4, dewets the surface regardless of the length scales of the heterogeneities. PS is expected to dewet on a surface comprised of P(S-*r*-MMA) and PS that has been oxygen plasma treated and UV exposed. However, after 2 h of annealing at 170 °C, the characteristics of the dewetting film are seen to depend strongly on the length scale of the heterogeneities. Such behavior has been seen previously by Quéré and co-workers,[26] McCarthy et al.,[27] and others[28] where, by varying the length scales of surface topographies, surfaces can be made ultrahydrophobic or superwetting, depending upon the spreading coefficient of the fluid on a perfectly smooth surface. In the example shown here, PS is seen to form isolated islands that are micrometers in size and the droplets form polygonal patterns at the intermediate region. This, as discussed by Reiter et al.,[29] results from the impingement of dewetting fronts that have been randomly initiated across the film. Such behavior is, for example, seen for PS on a silicon oxide surface. Decreasing the length scale of the heterogeneities further, to the nanoscopic level, the number of sites where dewetting has nucleated is significantly depressed and only isolated dewetting sites are evident. This result suggests that, as the size scales of the heterogeneities decrease, the ability of the PS film to sense the underlying P(S-*r*-MMA) substrate decreases. The PS is not able to wick between the oxygen plasma treated PS topographical features on the surface and reduces contact with the exposed P(S-*r*-MMA) substrate. Thus, the PS homopolymer effectively bridges from one oxygen plasma

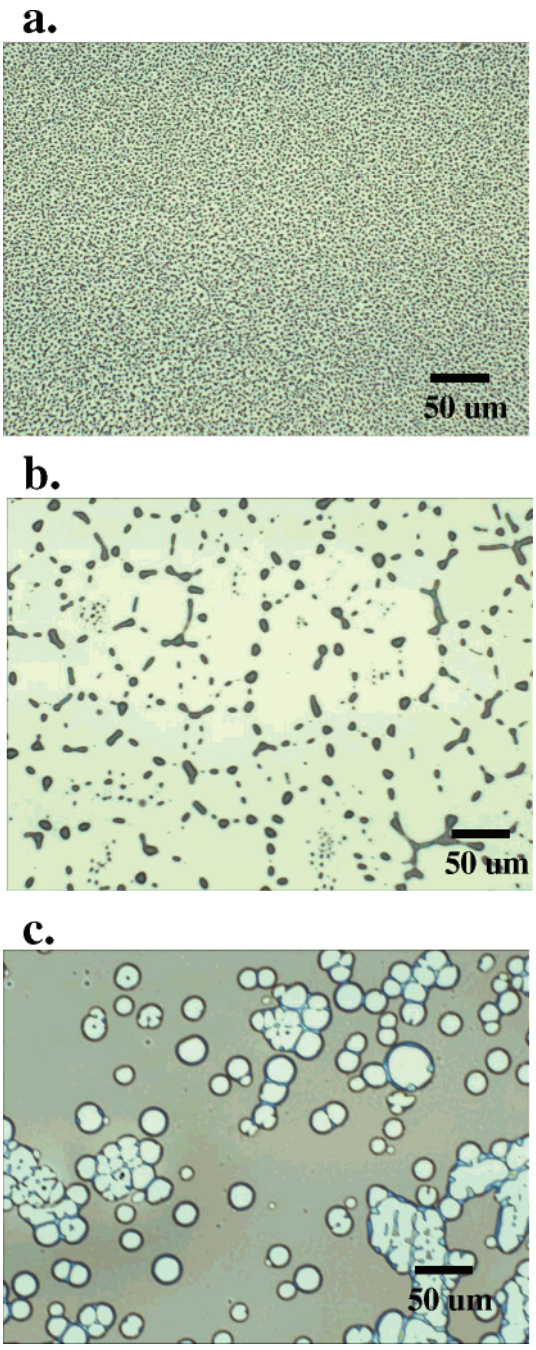

Figure 4. Dewetting of a 30 nm thick PS film on a (a) microscopic area, (b) intermediate area, and (c) nanoscopic area of gradient heterogeneous surfaces at 2 h of annealing at 170 °C.

treated PS feature to the next. As the size scales increase, such bridging is not feasible and the PS homopolymer dewets the P(S-*r*-MMA) and rests on the oxygen plasma treated PS surface feature. On the micrometer length scale, uniform dewetting droplets are formed without the formation of polygon patterns. This suggests that the initial hole growth is not random but rather biased by the micrometer-sized domains. In fact, it appears as if the dewetting droplets conform to the micrometer-sized patterns on the surface.

The phase separation on chemically heterogeneous surfaces with topography involves a combination of phase separation, wettability, and capillarity. Numerous studies have appeared dealing with the phase separation of thin

(26) Bico, J.; Tordeux, C.; Quéré, D. *Europhys. Lett.* **2001**, *55* (2), 214.
(27) Oner, D.; McCarthy, T. J. *Langmuir* **2000**, *16*, 7777−7782.
(28) Onda, T.; Shibuichi, S.; Satoh, N.; Tsujii, K. *Langmuir* **1996**, *12*, 2125.
(29) Reiter, G. *Phys. Rev. Lett.* **1992**, *68*, *1*, 75.

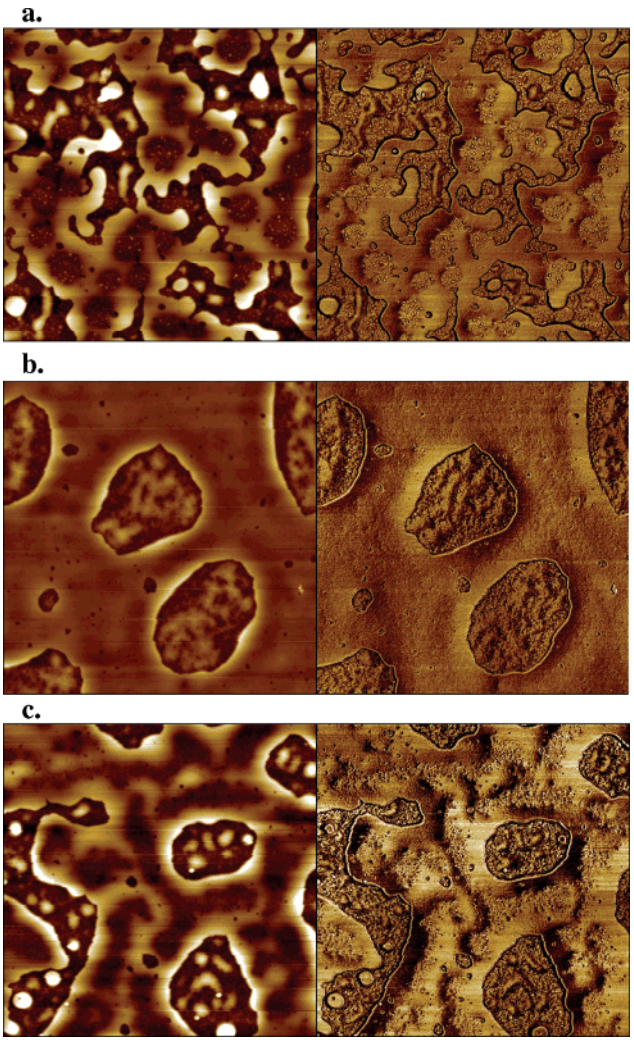

Figure 5. Thin film of PS (52K) + PMMA (29K) on a (a) microscopic area, (b) intermediate area, and (c) nanoscopic area of a gradient heterogeneous surface annealed at 170 °C for 24 h and washed with cyclohexane. Each AFM image is $5 \times 5\ \mu m^2$ of the height (left) and phase (right) images. The height and phase scales range between 0 and 80 nm and 0° and 20°, respectively.

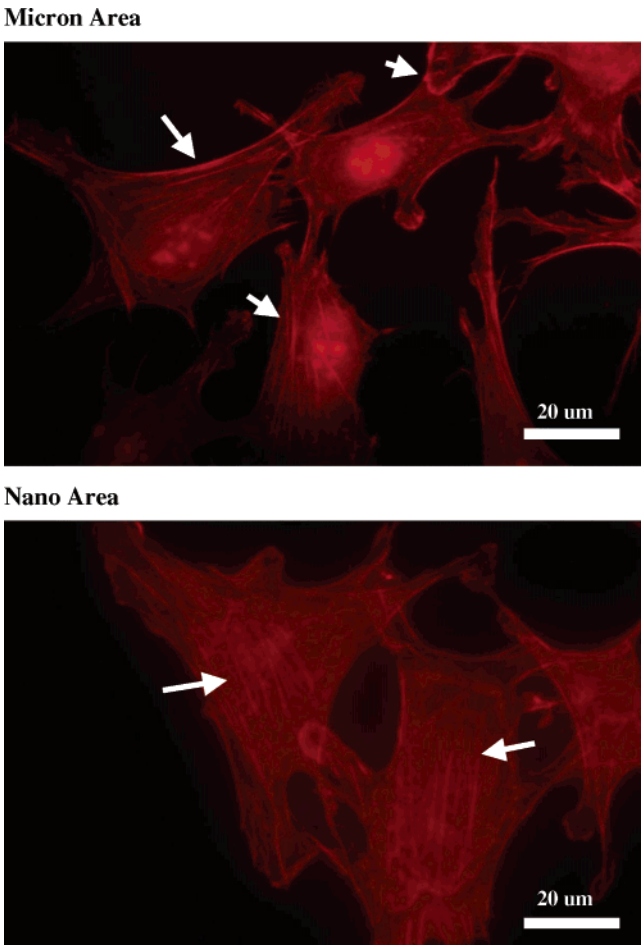

Figure 6. Fluorescence microscopic images of fibroblasts NIH3T3 on gradient heterogeneous surfaces after 2 h.

film polymer blends on homogeneous surfaces[30,31] and on chemically patterned substrates.[1−4] Krausch et al.[1] and Böltau et al.[3] observed the formation of periodic stripelike domains of PS and brominated PS on micrometer-sized periodic stripes of a Cr- and hydrogen-passivated surface and PS and poly(vinylpyridine) on a micrometer-sized periodic array formed by alternating stripes of Au and self-assembled monolayers (SAMs) of an octadecyl merctaptan pattern, respectively, indicating a surface-directed spinodal decomposition. As the size scales of the patterns decrease to ~60 nm of patterned substrate, Rockford et al.[18] found the polymer blend macroscopically phase separated as if on a homogeneous neutral surface. However, immediately adjacent to the surface, phase separation on the nanoscopic level was observed. In Figure 5, macrophase separation is seen from the microscopic to the nanoscopic length scale after annealing at 170 °C for 24 h and washing with cyclohexane, a selective solvent for PS. This implies that the chemical heterogeneities of oxidized PS and P(S-*r*-MMA) do not appear to play a major role in directing the phase separation, but the topography has a strong influence on the morphology of mixtures in thin films. A striking observation is the boundaries between the PS and PMMA domains. These wavy contact lines on heterogeneous surfaces have been theoretically treated by Swain and Lipowsky[32] for wetting phenomena of a rough and chemically heterogeneous surface.

The oscillation of the contact line between PS and PMMA is observed regardless of the length scale of the surface heterogeneities. However, the fluctuations at the PS and PMMA interface is significantly more pronounced in the case of surfaces where the heterogeneities are on the micrometer length scale. This agrees with the concept that larger heterogeneities give larger fluctuations of the contact line. For surfaces with a smaller length scale of heterogeneities, the energetic cost of having the increased surface area is too high and the phase-separated morphology cannot follow the patterning. In addition, the morphology changes from holes at the intermediate region to a mixture of ribbons and holes on the nanoscopically heterogeneous surface. This suggests that coarsening kinetics is suppressed as the lateral length scale of the surface heterogeneities decreases. It is evident that this results from an interplay among phase separation, dewetting, and capillarity of the thin film mixture.

Cell adhesion also shows distinct differences on gradient heterogeneous surfaces. Cells were found to align in the grooves when plated onto a chemically homogeneous surface with etched grooves and actin filaments within

(30) Jones, R. A.; Kramer, E. J.; Rafailovich, M. H.; Sokolov, J.; Schwarz, S. A. *Phys. Rev. Lett.* **1989**, *62*, *3*, 280.
(31) Bruder, F.; Brenn, R. *Phys. Rev. Lett.* **1992**, *69*, *4*, 624.
(32) Swain, P. S.; Lipowsky, R. *Langmuir* **1998**, *14*, 6772−6780.

the cells oriented parallel to the direction of the grooves.[9,10] This phenomenon is known as contact guidance. Moreover, cells react preferentially to chemical cues when attached to adhesive and nonadhesive patterns.[11−14] Cells on chemical heterogeneous surfaces and surfaces with roughness have been reviewed recently by Whitesides[12] and Flemming et al.,[10] respectively. In our example, both the chemistry and geometry of the surface have important consequences on how cells adhere and migrate on the gradient heterogeneous surfaces. Fibroblasts NIH3T3 spread more on a homogeneous surface of oxygen plasma treated PS than on a homogeneous surface of P(S-*r*-MMA). This is further evidenced by scanning electron microscopy showing preferential attachment of the pseudopods on the oxygen plasma treated PS. Since the patterns generated by homopolymer/diblock copolymer mixtures are randomly arranged on the surface with no specific orientation, the cells did not align with any preferred orientation. Although cells spread regardless of the size scale of the heterogeneities, the cells on surfaces with micrometer-sized heterogeneities are smaller than the cells on surfaces with nanometer-sized heterogeneities.

Shown in Figure 6 are fluorescence microscopic images of cells plated on the surface for 2 h, fixed and stained to visualize the cytoskeleton structures. Cells on the micrometer-patterned surface have few axial stress fibers, and most of the F-actin is located at the cell periphery and at the cell membrane. Cells on the nanometer size patterned surface have a large number of axial stress fibers, but they are not elongated into axial stress fiber supported filopodia. Specific details on the relationship between cell spreading area and actin filament formation and the lateral length scale of the heterogeneities will be discussed elsewhere. However, it is evident that surface topography and heterogeneities and the lateral length scales of each have a strong influence on the interaction of cells at surfaces.

Conclusion

By using phase separation of a homopolymer blend and microphase separation of a diblock copolymer, a gradient heterogeneous surface can be made where the lateral length scales of the heterogeneities vary from microscopic to nanoscopic. It has been shown that phenomena ranging from wetting to phase separation to cell adhesion depend strongly on the lateral length scale of the heterogeneities. The results shown on gradient surfaces clearly show an optimal length scale for each of these processes. Therefore, by manipulating the size scale, the surface patterns can be tuned to meet a specific application. Gradient surfaces provide a simple and direct means of assessing this length scale optimization.

Acknowledgment. Funding for this work was provided by the U.S. Department of Energy and MRSEC (Material Research Science and Engineering Center).

LA049957W